Article:

Dizayi, B, Li, H, Tomlin, AS et al. (1 more author) (2014) Evaluation of the effect of fuel properties on the fuel spray and jet characteristics in a HGV DI diesel engine operated by used cooking oils. Applied Mechanics and Materials, 694. 3 - 12. ISSN 1660-9336

https://doi.org/10.4028/www.scientific.net/AMM.694.3

Evaluation of the Effect of Fuel Properties on the Fuel Spray and Jet Characteristics in a HGV DI Diesel Engine Operated by Used Cooking Oils

Buland Dizayi, Hu Li, Alison S. Tomlin and Adrian Cunliffe

Energy Research Institute, University of Leeds, Leeds, UK.

pmbid@leeds.ac.uk or fuehli@leeds.ac.uk

Keyword: fuel spray, SMD, HGV, diesel engine, biofuel, used cooking oil

ABSTRACT

Fuel injection systems in modern diesel engines are designed and built to comply with very stringent environmental standards. They should also meet the highest level of fuel economy. Drivability, rapid response and easy and accurate control are a common demand. Changing the fuel characteristics could affect the performance of the fuel injection system. This study focuses on the evaluation of fuel spray characteristics of straight used cooking oil (SUCO) and its blends with petroleum diesel (PD) as a surrogate for pure PD. Used cooking oil blends have quite different physical properties from those of pure PD. Data for the lower heating value (LHV), density and viscosity were obtained from laboratory analysis. These data were merged with the physical and thermodynamic conditions of the diesel engine of interest to evaluate the dynamic behaviour of the fuel jet in 360° of crank rotation namely, the compression stroke, and the power stroke including the injection process. Engine operational conditions were calculated using a diesel dual thermodynamic cycle taking into account fuel injection adjustment at three different speeds, namely, idle speed, maximum torque speed and rated power speed.

The results showed that fuel jet characteristics vary with SUCO content in the fuel blend. Two ranges of SUCO content in the blends were distinguished, 0 – 80% SUCO content and 80 – 100% SUCO content. Both showed a constant rate of change of jet characters per 10% increase in SUCO content in the fuel blend. Lower rates of change of fuel characters were observed at 0-80% SUCO content. The higher the temperature, the lower the rate of change of fuel jet characteristics.

1. INTRODUCTION

The engineering and geological estimations revealed by British Petroleum (BP) in 2012 stated that there was a growth in proved oil reserves since the 1980s. However oil prices started to increase rapidly during the same period [1].

Heavy goods vehicle (HGV) fleet operators have a desire to use cheaper surrogate fuels than petroleum diesel (PD) as cost is one of their important operating parameters. HGVs are also a significant contributor to road transport CO_2 emissions.

To maximize carbon reduction potential, the EPID (Environmental and Performance Impact of Direct use of used cooking oil in trucks under real world driving conditions) project has been set up to examine and investigate the environmental and performance impacts of the direct use of refined straight used cooking oils in diesel engine powered 44 ton trucks. A used cooking oil derived biofuel, C2G (C2G: Convert to Green) Ultra Biofuel (hereinafter known as UBF) is a fully renewable fuel made as a diesel replacement from processed used cooking oil, used directly in diesel engines. A dual fuel tank containing the UBF and PD has been fitted to the truck. Twelve fuel samples were collected, analysed and grouped into four seasonal batches. Both neat and blends of the UBF with PD were investigated. The aim of this paper is to evaluate the fuel jet properties of the UBF and its blends with PD as surrogate fuels in a Mercedes Benz Axor-C 2543 tractor engine in comparison to those of conventional pump PD. The study emphasises the properties of viscosity, density and lower heating value of the UBF and its blends with PD on the jet characteristics such as penetration length, Sauter Mean Diameter (SMD), fuel jet cone angle and jet velocity at different engine speeds and injection timings taking into account the piston crown cavity size as a limit for the maximum jet penetration length.

2. FUEL SPRAY AND KEY PARAMETERS AFFECTING ITS PERFORMANCE

Many researchers [2],[3],[4],[5] and [6] performed experimental studies to visualise and model the fuel jet behaviour in a confined steady state environment. The models include semi empirical equations for the fuel jet characteristics. Pastor et al [7] used an optically accessible cylinder head engine to find the best correlation between the fuel properties and the varying physical circumstances in the cylinder. Martinez et al [5] used a similar technique with various injection pressures ranging from 300 to 1300 bar. They used a single axisymmetric-hole mini-sac nozzle with diameter range from 115 to 200μm.

The fuel jet penetration length S can be defined as the maximum distance for the fuel jet to extend before reaching the walls of the combustion chamber. A model was developed by Wakuri et al [8] based on momentum theory neglecting the relative motion between the fuel droplets and the surrounding air giving:

$$\boldsymbol{S = 1.189\, C_d^{0.25} [\frac{\Delta P}{\rho_g}]^{0.25} [\frac{d_o t}{\tan \alpha}]^{0.5}} \quad \ldots\ldots\ldots\ldots \quad (1)$$

where, ΔP is the pressure drop across the nozzle opening in [Pa], d_o is the nozzle outlet diameter, α is the fuel jet cone angle and ρ_g is the gas density.

C_d is the coefficient of discharge for the nozzle opening which can be found by the following equation proposed by Dernotte et al [2].

$$\boldsymbol{C_d = 1 - 5.26\, \upsilon_f^{-0.06} . \Delta P^{-0.73} - \left[\frac{-400 \upsilon_f^{-0.74} . \Delta P^{-0.51}}{Re^{0.54}}\right]} \quad \ldots\ldots\ldots\ldots \quad (2)$$

where, υ_f is the fuel kinematic viscosity and ΔP is in [MPa]. The Reynolds number Re is given by

$$\boldsymbol{Re = \frac{V_{th} . d_o}{\upsilon_f}} \quad \ldots\ldots\ldots\ldots.. \quad (3)$$

and V_{th} is the theoretical fuel velocity issuing from the nozzle opening [m/s]:

$$\boldsymbol{V_{th} = [\frac{2\, \Delta P}{\rho_f}]^{0.5}} \quad \ldots\ldots\ldots\ldots \quad (4)$$

with ρ_f the fuel density and ΔP is in [Pa].

Sauter Mean Diameter (SMD) is defined as the mean diameter of the jet droplets that have the same surface area to volume ratio. Dernotte et al. [2] proposed (eq.5) for SMD measurement at very high injection pressures:

$$\boldsymbol{SMD = 9.57 . V_{act}^{-0.37} . \rho_g^{0.21} . \rho_f^{0.28} . e^{0.03 \upsilon_f}} \quad \ldots\ldots\ldots.. \quad (5)$$

where, V_{act} is the actual fuel jet velocity in [m/s] (defined in eq.7 below).

Agarwal and Chaudhury [6] defined the spray cone angle α as the largest angle formed by two straight lines from the nozzle hole to the spray boundary. Dernotte et al.[2] proposed the following equation for the determination of fuel jet cone angle:

$$\boldsymbol{\tan \frac{\alpha}{2} = 0.24\, [\frac{\rho_g}{\rho_f}]^{0.24} . \Delta P^{0.08} . e^{-0.24\, \Delta P^{-0.58} . \upsilon_f}} \quad \ldots\ldots\ldots \quad (6)$$

with ΔP in [MPa] and

V_{act} is the actual initial fuel velocity issuing from the nozzle opening.

$$\boldsymbol{V_{act} = C_d\, V_{th}} \quad \ldots\ldots\ldots.. \quad (7)$$

Demirbas [9] proposed the following correlation between the kinematic viscosity and density of vegetable oils with a coefficient of regression of $R^2 = 0.9398$:

$$\boldsymbol{\upsilon_f = -0.7328 \rho_f + 938.57} \quad \ldots\ldots\ldots\ldots \quad (8)$$

A higher fuel viscosity could reduce the spray cone angle and increase the penetration length and it could reduce the fuel flow rate due to the increased friction coefficient [3].
Demirbas [9] suggested the following equation as an easier, faster and cost effective way for higher heating value (HHV) determination for vegetable oils with a coefficient of regression of R^2= 0.9435:

$$\boldsymbol{HHV = 0.0317\upsilon_f + 38.053} \qquad \ldots\ldots\ldots\ldots \quad (9)$$

3. SPECIFICATION OF ENGINE, FUEL BLENDING SYSTEM AND FUEL PROPERTY MEASUREMENT METHODS

3.1. The Engine to be simulated for Fuel Spray Properties

The targeted test vehicle is powered by a Mercedes Benz engine with specifications as in table 1.

Table 1: The specifications of the targeted engine to be simulated.

Engine parameter or physical quantity	Units	Value
Engine model	OM 457 LA EURO 5	
No of cylinders		6 in line
Displacement	[Litre]	11.97
Bore	[mm]	128
Stroke	[mm]	155
Connecting rod length	[mm]	≈250
Piston crown cavity volume	[cm^3]	93.6
Compression ratio		18.5
Engine compartment temperature(max permissible)	[°C]	100
Rated power	[kW]	315 at 1900 rpm
Maximum torque	[Nm]	2100 at 1100 rpm
Low idle speed, standard	[rpm]	560
Cooling system thermostat start to open at	[°C]	83
Charge air pressure after turbocharger at rated power	[bar]	1.9
Charge air pressure after turbocharger max.	[bar]	1.9
Charge air temperature before engine	[°C]	41
Fuel injectors	6 Electronic controlled unit injectors centrally positioned in the cylinder head	
Injection pump	6 single injection pumps integrated in the crank case	
Maximum injection pressure	[bar]	1800
Number of injection holes	-	7
Injector hole diameter	[μm]	200
Maximum permissible fuel jet length	[mm]	≈48
Maximum permissible air temp at rated power	[°C]	55
Exhaust gas temperature (max.)	°C	530

Courtesy of Daimler Chrysler AG, D-70546 Stuttgart/ Germany.

The data in table 1 were used in the Diesel dual cycle for a close simulation of the injection environment including the dynamic variation of in-cylinder gas pressure, temperature and density at different speeds taking into account the differences in LHV and injection timing adjustment due to speed variation.
The tests were carried out at the standard low idle speed, the maximum torque speed and the rated power speed. A P-V diagram was plotted for the combined data of engine characteristics and fuel properties. Special attention was paid to the range of crank angles between (20° bTDC to 20° aTDC with increments of 2.5°CA) where the injection process takes place.

3.2. On-board fuel blending-Bioltec System

An on-board fuel blending system-Bioltec system was installed in the vehicle fuel system to enable heating the UBF and automatic determination of the required blending ratio between diesel and the UBF depending on engine conditions. Data collected from the Bioltec system for a real world driving test between Ashby De La Zouch and Wigston were analysed. The data revealed that the system allows the UBF to be delivered to the engine only at fuel line temperatures higher than 45°C up to the maximum engine compartment temperature.

3.3. The UBF Sample property measurement

The density of the fuel blends were measured manually using a 5 ml Pychnometer. The tests were carried out at 23°C and then all the data were adjusted to temperatures ranging from 15°C to 100°C (fuel system operational temperatures) according to the correlation equations based on API-ASTM-IP (ISO 91-1).
The viscosity of the fuel blends were measured in a variable temperature test using a Bohlin Rheometer, (Malvern Instruments). The temperature range covered by this test was (15-110°C).

The HHV of the UBF was obtained by Bomb Calorimetry. Parr 6200 Bomb Calorimeter was used for this purpose. In order to obtain the LHV of the fuel, CHNS analysis of the UBF was performed. A Flash EA2000 CHNS-O had been used to obtain the mass percentage of hydrogen in the UBF sample which was used in the LHV determination.

4. RESULTS

4.1. Variation of Fuel Density for Different Batches and Blends as a function of Temperature

Fig. 1 shows the variation of UBF and its blends with PD with temperature. The higher the UBF content in the blend the greater the ρ_f at a given temperature. The UBF is prohibited from entering the engine at temperatures lower than 45°C because its density is 8% higher than that of PD.

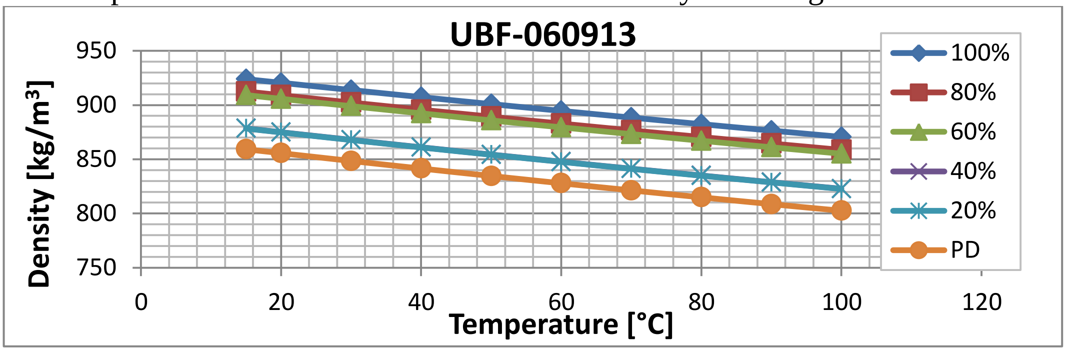

Figure 1 UBF Summer batch blend density variation with temperature in comparison with PD.

4.2. Variation of Fuel Viscosity for Different Batches and Blends as a function of Temperature

Fig. 2 shows that the kinematic viscosity of the blend increases dramatically as the UBF content in the blend increases even at high temperatures.

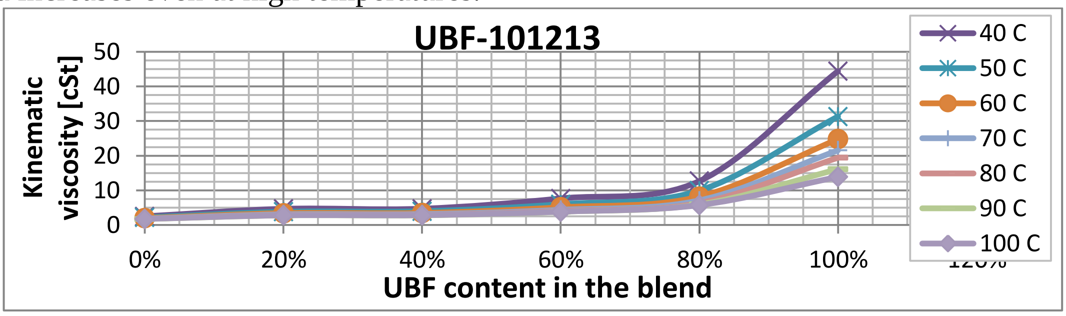

Figure 2 Variation of υ_f with UBF content in the blend at different temperatures.

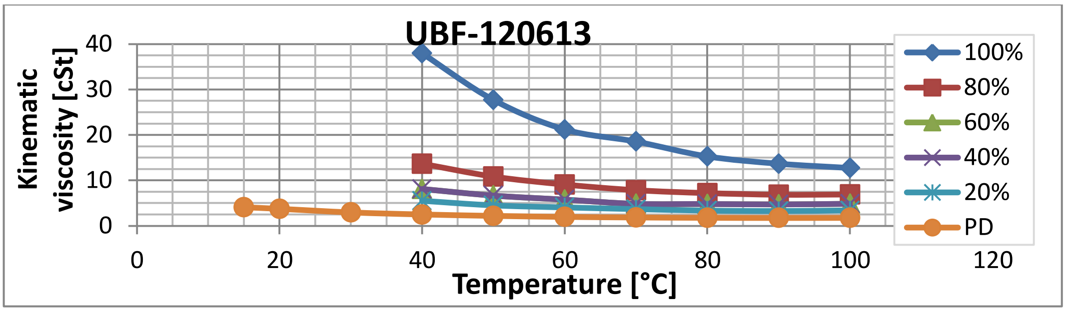

Figure 3 Variation of υ_f with temperature for different blends of the summer batch.

Fig. 3 shows that UBF is more sensitive to temperature variations than PD. Increasing the temperature from 40°C to 100°C reduces the υ_f of UBF to 35% of its original value, while υ_f for PD reduces to only 70% of its original value for the same temperature increase. However the kinematic viscosity of UBF is still sevenfold higher than that of PD at 100°C.

4.3. Fuel Jet Length

a

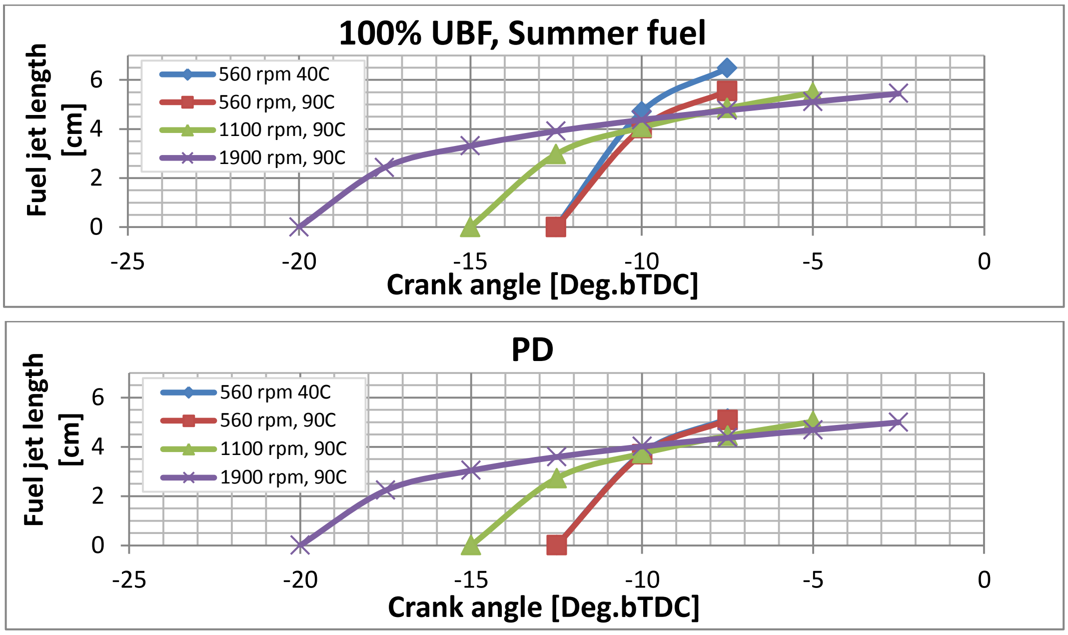

b

Figure 4 Variation of fuel jet length with crank angle for UBF and its blends in comparison to PD at different fuel temperatures and engine speeds.

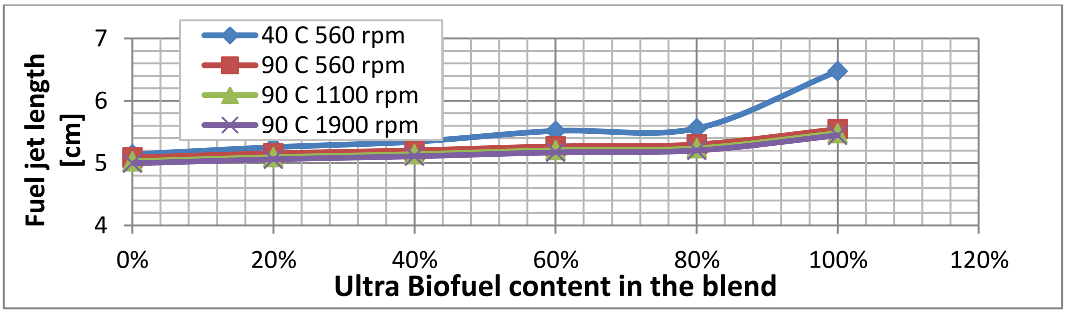

Figure 5 Variation of fuel jet length with UBF content in the blend for various engine speeds and fuel temperatures.

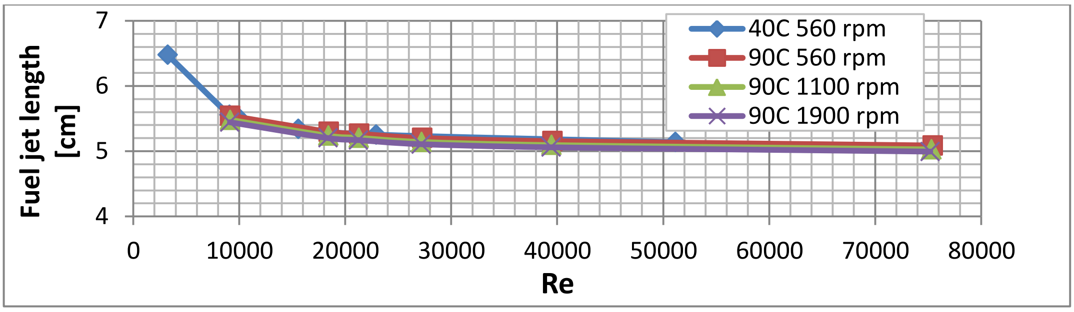

Figure 6 Variation of fuel jet length with Re at various engine speeds and fuel temperatures.

Fig. 4 illustrates the growth of the fuel jet in the combustion chamber from the start of the injection process to the maximum allowable distance the jet could travel before collision to the piston bowl wall which is about [5 cm]. It is observed that each curve exhibits two rate of jet growth. A high rate of fuel jet growth at the beginning is followed by a lower rate of growth towards the end. This could be attributed to the higher gas pressure and density as the piston ascends to its upper dwell. The graphs also show that, even with injection timing advancement, the rate of fuel jet growth at high engine speed is lower than that at the low speeds. This is affiliated to higher rate of gas pressure and temperature rise at higher speeds. A comparison among the fuel jet behaviours at different temperatures shows that the sensitivity to temperature variation is greater as the UBF content in the blend increases (Fig. 5). Therefore it is seen that pure UBF possesses a higher rate of growth (Fig. 4a) at 40°C than 90°C especially as the piston gets closer to the TDC. This is quite clear in Fig. 6 and could be attributed to the domination of the viscosity effects (larger droplets) to the inertia effects (lower velocity). Unfortunately this jet behaviour is a major cause of fuel-wall collision at an even earlier time. Practically, this might result in higher fuel consumption, more lube oil dilution, higher emissions and lower output power.

4.4. Fuel Droplet Size-SMD

Fig. 7 exhibits a slight increase in the fuel mean droplet size SMD with crank angle. This is an inevitable result of the decrease of the pressure difference ΔP between the injection pressure and the gas pressure. The gas pressure continues to increase as the piston gets closer to the TDC and after the combustion starts. The reduced ΔP adversely affects the atomisation process therefore larger droplets are found in the spray.

a

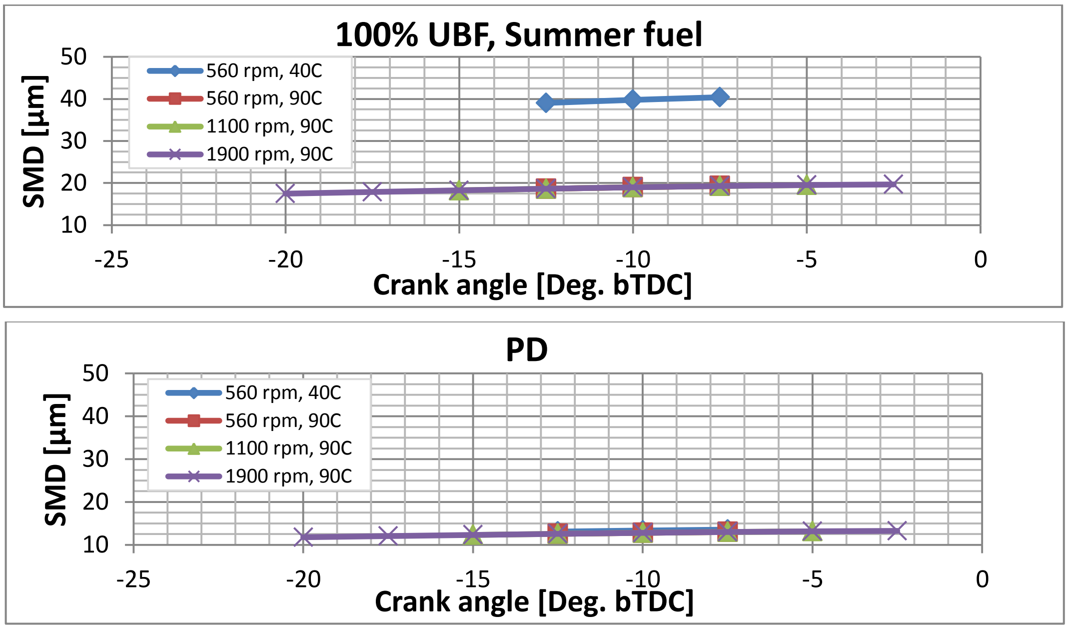

b

Figure 7 Variation of SMD with crank angle for UBF and its blends with PD at different fuel temperatures and different engine speeds.

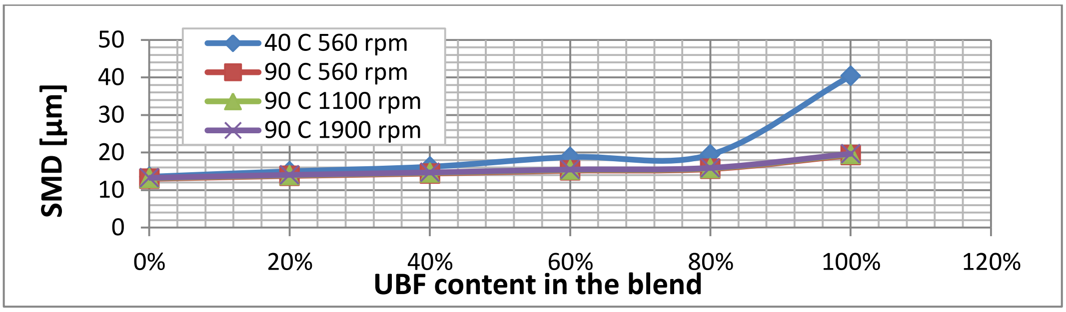

Figure 8 Variation of SMD with UBF content for various engine speeds and fuel temperatures.

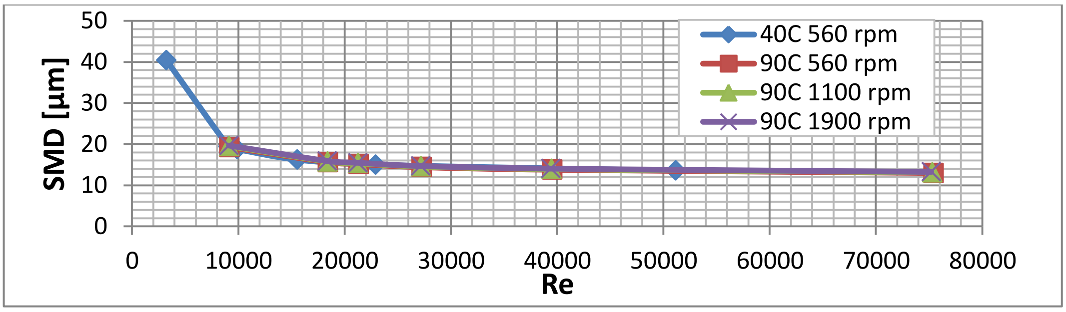

Figure 9 Variation of SMD with Reynolds number for various engine speeds and fuel temperatures.

Fig. 8 shows that larger fuel droplets are observed as the UBF content in the blend increases at a given crank angle especially at lower temperatures. Pure UBF at 90°C produces droplets with SMD half that of the same fuel at 40°C at the same operational conditions. It is also seen that at 90°C pure UBF produces fuel droplets with SMD 60% larger than that of the PD at a given operational condition.

Fig. 9 explains the phenomena, as the higher viscosity of UBF hinders the fuel flow, reduces the flow velocity and increases the droplet size. Therefore the viscous effect dominates even for the higher density of the UBF which is dampened by the low droplet velocity. The practical consequences for the larger SMD is a limited fuel to air contact and a greater temperature gradient from the surface to the centre of the droplet which affects fuel evaporation and mixing with air. A more heterogeneous mixture with longer ignition delay period is expected.

4.5. Fuel Spray Cone Angle

Fig. 10 illustrates the increase in the fuel jet cone angle as the fuel injection process gets close to the TDC. This could be attributed to the growing gas density which applies a high shear to the fuel jet, a high drag force on the jet front and a more air entertainment and mixing. It is also seen that increasing the UBF temperature from 40-90°C increases the jet cone angle by 34%. At 90°C the jet cone angle in PD is always 18% larger than that of UBF due to its lower viscosity and density and hence smaller SMD and jet length.

a 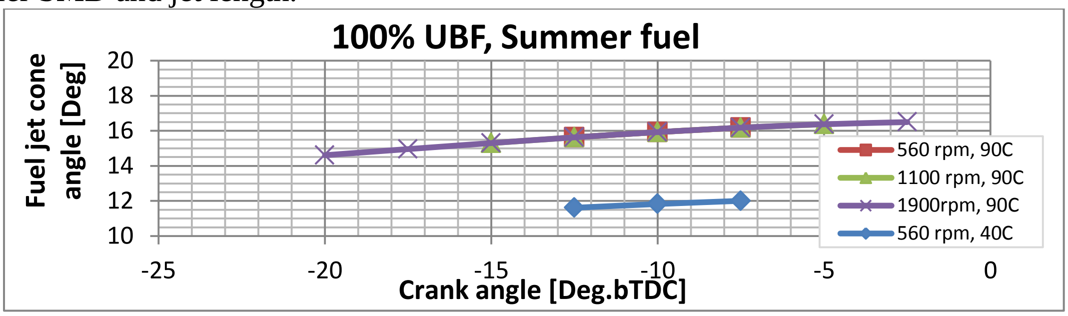

b 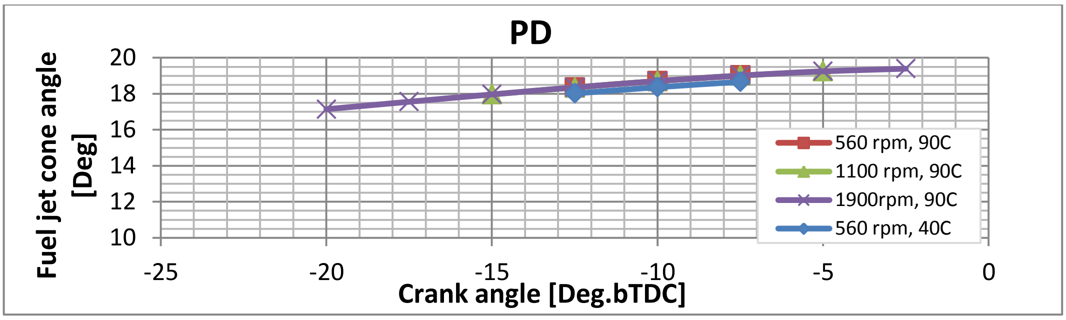

Figure 10 Variation of fuel jet cone angle with crank angle for various UBF blends at different engine speeds and fuel temperatures.

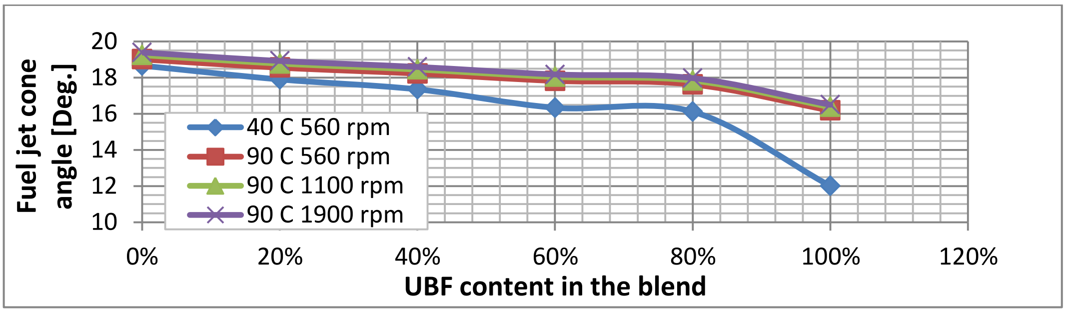

Figure 11 Variation of fuel jet cone angle with UBF content in the fuel blend at various engine speeds and fuel temperatures.

Fig. 11 shows that the fuel cone angle is inversely proportional to the UBF content in the blend especially at lower temperatures. This could be related to the prevalence of the viscosity effects (fig. 12) which increase the friction in the nozzle and reduce the jet velocity. Smaller fuel cone angle means that the fuel jet preserves the core structure and keeps the fuel droplets close to jet core for a longer time. This will reduce air entrainment to the fuel. The net effect is a deteriorated fuel atomisation towards a highly heterogeneous mixture. Here again the effect of UBF's higher density is opposed by the lower jet velocity.

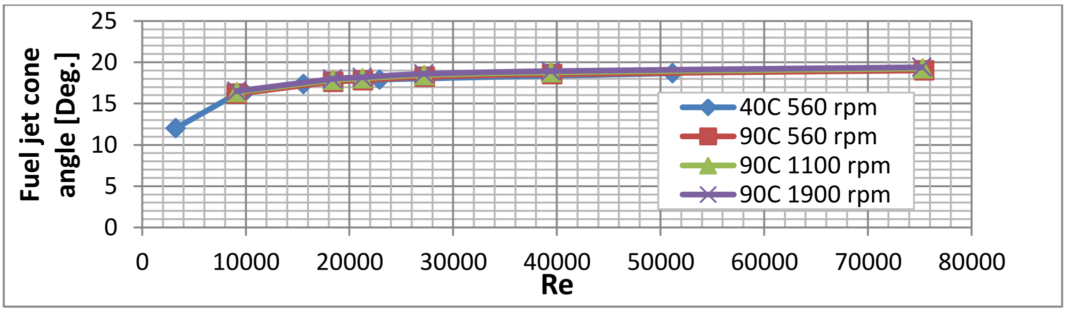

Figure 12 Variation of Fuel jet cone angle with Re at various engine speeds and fuel temperatures.

5. SUMMARY

The variations in physical properties of the fuel affect the fuel jet characteristics. The data in table 2 are taken at the same engine operational conditions and for the fuel jet before its collision to the piston crown cavity wall. It could be inferred from the data that the υ_f of UBF reduces by 65% while that of the PD reduces by 30% as the temperature increases from 40°C to 90°C. This means that UBF is more sensitive to temperature variations than PD. However, as a magnitude the υ_f of UBF is seven fold larger than that of PD at the higher temperature extreme.

Table 2 Variation of fuel properties with temperature and their effect on fuel jet characteristics.

T [°C]	Fuel type	$\Delta\upsilon_f$ [%] (%Change in fuel kinematic viscosity)	$\Delta\rho_f$ [%] (%Change in fuel density)	ΔS [%] (%Change in fuel jet length)	ΔSMD [%]	$\Delta\alpha$ [%] (%Change in fuel jet cone angle)	ΔV [%] (%Change in fuel jet velocity)
40 - 90	PD	-30.8	-3.9	- 0.98	- 4.06	+1.86	+2.02
	100% UBF	- 64	-3.4	-14.35	-52.2	+34.6	+1.64

Accordingly, poorer atomisation, evaporation and mixing with air is expected from the UBF at the lower temperatures. Therefore the engine ECU in conjunction with the Bioltec system usually compromises between the fuel temperature and the UBF content in the blend. Using UBF and its blends with the PD showed considerable variations in the fuel jet characteristics especially at high UBF content blends and at low temperatures. The variations in fuel jet characteristics for this particular engine under the specified operational conditions are tabulated in table 3. The data in table 3 indicates the change of fuel jet characteristics in percentage for each 10% increase in UBF content in the blend delivered to the engine at 40°C and 90°C respectively for a fully extended jet to its maximum allowable length.

Table 3 Variation in fuel jet characteristics per 10% increase in UBF content in the blend.

Temperature [°C]	UBF content [%]	SMD [%]	Fuel jet cone angle [%]	Fuel jet length [%]
40	0-80	5.42	-1.70	1.01
	80-100	77.35	-11.00	8.96
90	0-80	2.50	-0.91	0.52
	80-100	14.15	-3.80	2.42

The data shows that the variation of the fuel jet characteristics with UBF content could be classified into two ranges. The first one is the percentage change in spray characteristics for UBF content variation in the blend from 0-80%, which follows a nearly constant rate of change of jet characteristics, and the change in jet characteristics at 40°C is about twice those at 90°C.

The second range is the variation of UBF content in the blend from 80% to 100% (pure UBF) which shows a great difference in jet characteristics. Comparing the fuel jet characteristics for this range at 90°C with 0-80% shows that: the rate of increase of SMD is 5.5 times higher, the rate of cone angle decrease is about 4 times lower and the rate of jet length increase is 4.7 times higher. Performing the same comparison at 40°C gives the SMD increase, α decrease and S increase in the following sequence: 14.25, 6.45 and 8.84 respectively.

It could be concluded that engine speed has a negligible effect on the SMD and jet velocity, while the fuel temperature plays a key role in spray characteristics. Therefore it is more convenient to operate the engine on blends with UBF content up to 80% to avoid higher fuel consumption and higher pollution load on the exhaust after treatment system compared to using 100% UBF. Although the higher fuel viscosity deteriorates the combustion process and the engine output, the higher fuel density could compensate for the lower heating value of the UBF and to lower the expected increase in fuel consumption to obtain the same power output.

Acknowledgements

We would like to thank UK Department for Transport and Technology Strategy Board for supporting the research element within the project “Environmental and Performance Impact of Direct use of used cooking oil in 44 tonne trucks under real world driving conditions” which is part of the Low Carbon Truck Demonstration Trial [21].” Thanks go to United Biscuits Midland Distribution Centre for the provision of a truck and general support and collaboration in field tests. Thanks also go to Bioltec System GmbH for advice and permission to use some technical information and Convert2Green for the provision of UBF for the tests. Special appreciation and gratitude to the Iraqi MoHE&SR and the Iraqi Cultural Attaché/London for sponsoring the PhD program of the author.

References:

1. Morey, B., *Future automotive fuels and energy*. 1st ed. 2013, USA: SAE International. 93.
2. Dernotte, J., C.Hespel, F. Foucher, S. Houile, C. Mounaim-Rousselle, *Experimental study of the infuence of fuel physical properties on the diesel injection process in non-vaporizing conditions.* 24th European conference on liquid atomization and spry systems, Estoril, Portugal., 2011.
3. Cipolat D., D.V., *comparison of theoretical and experimental diesel and DME injection spray characteristics.* Fuel processing thechnology, 2013. **107**: p. 36-43.
4. Delacourt, E., B. Desmet, B. Besson., *Characterisation of very high pressure diesel sprays using digital imaging techniques.* Fuel, 2005. **84**: p. 859-867.
5. Martinez, S., F.A. Sanchez-Cruz., *Liquid penetration length in direct diesel fuel injection.* Applied Thermal Engineering, 2008. **28**: p. 1756-1762.
6. Agarwal, A.K., V.H. Chaudhury., *Spray characteristics of the biodiesel/blends in a high pressure volume spray chamber.* Experimental thermal and fluid science, 2012. **42**: p. 212-218.
7. Pastor J.V., J.M.G.-O., J.-G. Verva, B. Gimenez., *Fuel effect on the liquid-phase penetration of an evaporating spray undertransient diesel-like conditions.* Fuel, 2011. **90**: p. 3369-3381.
8. Y. Wakuri, M.F., T. Amitani, R.Tsuneya., *Studies on the penetration of fuel spray in a diesel engine.* Bulletin of JSME, 1960. **3**(9): p. 129-130.
9. Demirbas, A., *Relationships derived from physical properties of vigitable oil and biodiesel fuels.* Fuel, 2008. **87**: p. 1743-1748.